

## Properties of Iron Powder for AC Magnetic Application

D. Rodrigues<sup>1</sup>, F.J.G. Landgraf<sup>1</sup>, M. Emura<sup>1</sup>, A.F. Flores Filho<sup>2</sup>, L.T Loureiro<sup>2</sup>  
and L. Schaeffer<sup>3</sup>

<sup>1</sup> Laboratory of Powder Metallurgy and Magnetic Materials, IPT, Universidade de São Paulo,  
Av. Prof. Almeida Prado 532, CEP 05508-901 São Paulo SP, Brazil

<sup>2</sup> Electrical Machines Laboratory, UFRGS, Av. Osvaldo Aranha 103, Porto Alegre 90035-190,  
Brazil

<sup>3</sup> Metal Forming Laboratory, Universidade Federal do Rio Grande do Sul, UFRGS,  
Av. Bento Gonçalves 9500, Porto Alegre 91540-000, Brazil

**Keywords:** Electrical Steels, Insulated Powder, Iron Powder, Magnetic Properties

**Abstract:** Insulated iron powders offer new possibilities regarding AC electrical machines performances. A trend in the electrical motor market is the variable speed model, to be used, for example, in compressors for air conditioning and refrigeration. The constant performance of the iron insulated powders over a wide frequency range and the three dimensional flux carrying capability are two key differences compared to conventional laminated assemblies. Magnetic properties of pressed and heat-treated iron insulated powders (Hoeganaes – SC100) are presented and discussed. Variables such as compaction pressure and heat treatment temperature were investigated. Properties such as density, green strength, electrical resistivity, permeability (for different frequencies) coercive force and losses were measured. A discussion considering eddy current and hysteresis losses is also presented. Results showed that the consolidation process (compaction and heat treatment) defines magnetic properties.

### Introduction

Powder metallurgy is a well-established process to produce soft and hard sintered magnetic materials [1]. Markets utilizing sintered soft magnetic P/M materials are restricted to DC applications. The idea to insulate magnetic particles to improve AC applications is not new [2], but the recent development of new iron powders with better compressibility and new coating technologies is nowadays increasing the interest in the production of micro-encapsulated composites [3,4,5].

### Experimental Procedures

The insulated powder used here was SC100 from Hoeganaes [1], which mentions 0.75% resin. Hoeganaes catalog mentions that densities of 7.45 g/cm<sup>3</sup> are reached by warm compaction at 690 MPa and 175 °C. Here the powder was cold pressed with different pressures and later heat treated at different temperatures. Three different sample types were produced: 31.7x12.7x6.35 mm<sup>3</sup> for transverse rupture strength test specimen; 50x10x6.5 mm<sup>3</sup> for electrical resistivity measurements; and 50x42x2.2 mm<sup>3</sup> rings for magnetic measurements. Fig. 1 presents the compressibility curve of the powder, for transverse rupture strength specimens. Density values, in the green and heat treated conditions, are presented in Table 1, showing that different sample sizes lead to slightly different densities, for the same compaction pressure.

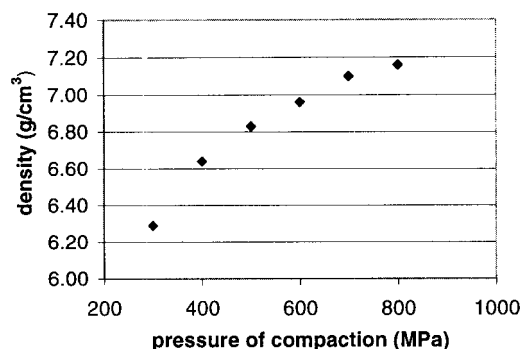


Fig. 1 Effect of compaction pressure on green density

Table 1 – Density in  $\text{g/cm}^3$  as a function of compacting pressure in the green and heat-treated ( $230^\circ\text{C}$ ) state, considering the three different specimen sizes.

pressure (MPa)	sample for electrical resistivity		sample for rupture strength		sample for magnetic measurements	
	pressed	treated	pressed	treated	pressed	treated
700	7.15	7.08	7.15	7.10	6.94	6.93
800	7.20	7.15	7.19	7.17	6.90	6.94
900	7.25	7.22	7.26	7.24	7.22	7.14

Transverse rupture strength was measured following ASTM B528. Resistivity was measured with the four terminal method, and magnetic measurements were performed following ASTM A596 method, and it was carried out by mathematical processing of current in the primary winding of the ring and the voltage in the secondary winding of the ring. Measurements at 400Hz were made maintaining sinusoidal induction.

## Results and discussion

Fig. 2 shows the effect of compaction pressure on electrical resistivity, for samples treated at  $150^\circ\text{C}$ . At lower compaction pressures the contact between particles is weak so resistivity is quite high. A resistivity plateau was found between 600 and 800 MPa.

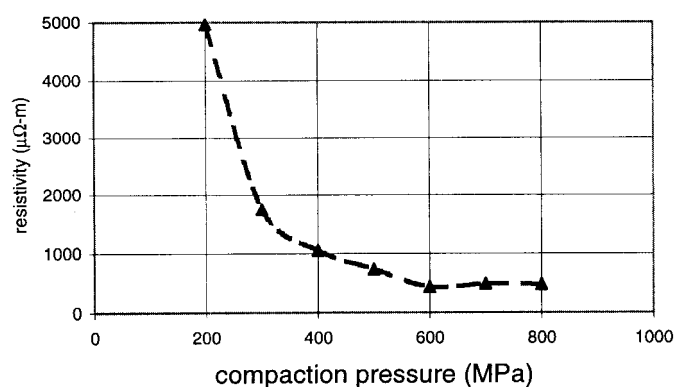


Fig. 2 – Electrical resistivity versus compaction pressure after heat treatment at  $150^\circ\text{C}$ .

Fig. 3 shows the effects of heat treatment temperature on electrical resistivity and transverse rupture strength of samples pressed with 700MPa. Resistivity decreases as temperature is increased, but peak values were obtained around 230°C. This behavior can be related to a possible polymer melting and polymer degradation at higher temperatures. Rupture strength shows a broad maximum around 300°C. Gélinas and Battison [3] mentioned a monotonic decreasing trend for resistivity, from  $250\mu\Omega\cdot\text{m}$  at 150°C to less than  $5\mu\Omega\cdot\text{m}$  at 500°C for powder with 0.8% resin pressed at 620 MPa.

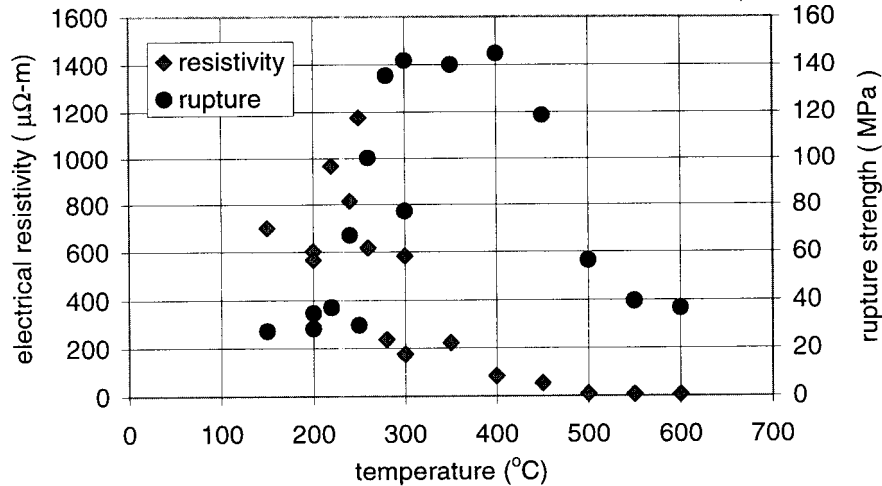


Fig. 3 – Electrical resistivity and transverse rupture strength versus heat treatment temperature.

Fig. 4 shows that transverse rupture strength increases with increasing density, but it was more sensitive to heat treatment temperature. The heat treatment at 150°C showed a very small strength improvement, but at 230°C the strength more than doubles, reaching values similar to those mentioned by Hanejko et al [1].

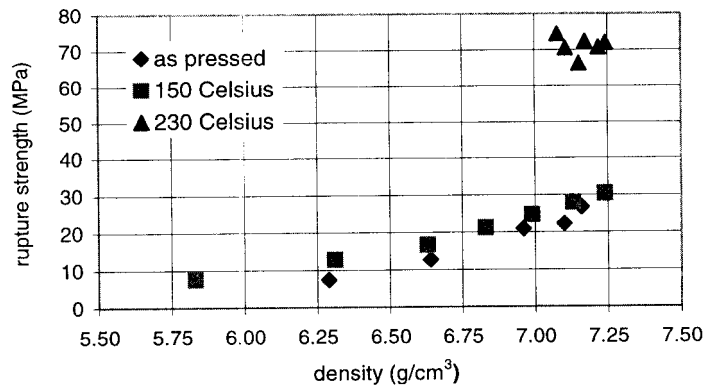


Fig. 4 – Rupture strength as a function of density for as pressed and heat treated at 150 and 230°C.

Fig. 5 shows DC magnetization curves for samples pressed at 700, 800 and 900 MPa, heat-treated at 230°C. The similar values for the 700 and 800MPa samples and the higher values of the 900MPa sample can be explained by the density behavior (see table 1). The positive effect of density increase on permeability is stronger than the expected from an increase in saturation magnetization: a 3% increase in density resulted in a 10% increase in magnetization, at 5 kA/m. The roles of the pores have to be further investigated. This may be the reason behind the much better values mentioned by Hanejko et al [1]. They reached 1.1 T at 3.2 kA/m. Fig. 6 shows hysteresis curves at DC and 400Hz. The very low values of remanence may be related to the plastic deformation induced by compaction and by the air gap effect (pores and coating).

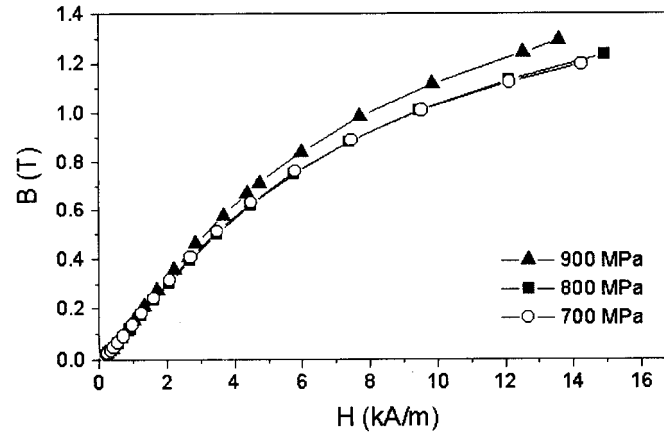


Fig. 5 – DC magnetization curves considering compaction pressure. Samples treated at 230 °C.

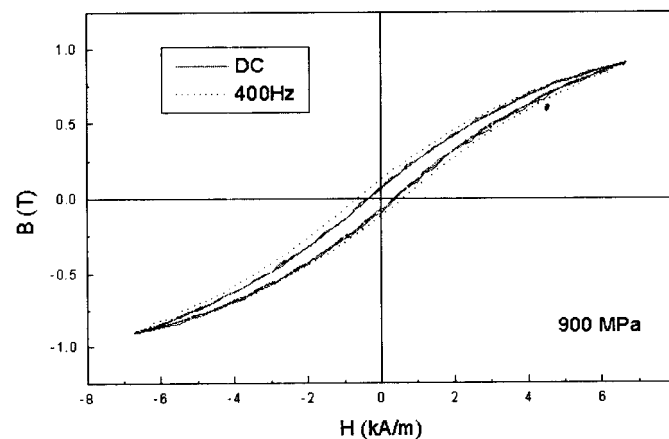


Fig. 6 – Hysteresis curves for samples treated at 230 °C.

Table 2 shows that the compaction pressure from 700 to 900 MPa did not change significantly the magnetic properties of sample heat-treated at 230°C. Resistivity was not as high as those observed in Fig. 3, indicating a strong sensibility to heat treatment. The hysteresis loss component found for the samples is very large. The average value of 70 W/kg should be compared to that of 0.21 mm Fe3%Si steel sheets, of approximately 5.2W/kg, at 1.0T and 400Hz. The total loss of this steel (1.0T, 400Hz) can be estimated as 14 W/kg [6]. It is interesting to discuss the loss behavior of the samples.

Table 2 - Magnetic properties of samples pressed at different pressures and heat treated at 230°C. Coercivity and losses were determined at 1,0T.

Pressure [MPa]	Resistivity [ $\mu\Omega\text{m}$ ]	DC			400Hz, 1,0T		
		$\mu_{\text{max}}$	$H_c$ [kA/m]	loop area [ $\text{J/m}^3$ ]	$H_c$ [kA/m]	Hyst. Losses [W/kg]	Total Losses [W/kg]
700	320	120	0.38	1180	0.65	68	106
800	300	117	0.39	1250	0.69	72	110
900	270	128	0.33	1230	0.63	69	99

The AC total losses can be divided in three components: the hysteresis component, the classic parasitic loss, and the anomalous parasitic loss.

The hysteresis loss can be calculated based on the DC hysteresis loop area ( $\text{J/m}^3$ ), multiplied by the frequency and divided by density to find it in W/kg. The classic parasitic loss ( $P_p$ ) can be estimated according to the equation (1):

$$P_p = \frac{(\pi * B * f * e)^2}{6 * d * \rho} \quad (1)$$

$P_p$  is the classic parasitic loss, taking into account the maximum induction  $B$ , frequency  $f$ , thickness  $e$ , density  $d$  and resistivity  $\rho$ . The constant  $\pi^2/6$ , valid for plates, must be substituted for  $\pi^2/20$  when estimating classic parasitic losses in spheres.

The anomalous parasitic loss is the difference between the total loss and the sum of hysteresis and classic parasitic loss.

Assuming 1.0 T, 400 Hz, sample thickness of 2.2 mm, density of  $7000 \text{ kg/m}^3$  and electrical resistivity of  $500 \mu\Omega\text{-m}$ , we get a  $P_p$  of 0.4 W/kg. This value is extremely low. For comparison, the 1.0T, 400Hz parasitic loss of the mentioned Fe3%Si steel can be estimated as 3 W/kg. The low value for the insulated iron powder is achieved through its very high resistivity, 1000 times larger than the value for silicon iron sheets. One may argue that the classic parasitic loss is occurring inside the iron particles, where resistivity is larger. The average particle size is  $80 \mu\text{m}$ , its density is  $7850 \text{ kg/m}^3$  and resistivity is  $0,1 \mu\Omega\text{-m}$ . Using these values we got 0,6W/kg, again too small. Some particles should be interconnected, so the “effective particle size” may be much larger than the particle size. Assuming, as a boundary case, that anomalous parasitic losses are negligible, we may calculate the “effective interconnected spherical particle size” based on equation (1) using  $P_p=P_T$ .  $P_H=105-70=35 \text{ W/kg}$ . We got  $590 \mu\text{m}$ .

Nevertheless, we cannot consider anomalous losses negligible. In the case of the 3%Si steel, we estimated values around 5.8 W/kg, which is larger than the hysteresis loss. G. Bertotti proposed that it is possible to calculate the anomalous loss, and the equation below is one of its versions, adapted from ref. [6]:

$$P_A = 8 \cdot B_{\text{max}} \cdot f \cdot GS \cdot (2 \cdot G^w \cdot \langle J_s \rangle \cdot H_{\text{hist}} \cdot f)^{1/2} / d \cdot \rho^{1/2} \quad (2)$$

$P_A$  is anomalous losses, W/kg

$B_{\text{max}}$  is the maximum induction. 1.0 T in this case

$f$  is frequency, 400Hz

$GS$  is grain size, here estimated as  $0.00004 \text{ m}$

$\rho$  is the electrical resistivity,  $10^{-7} \Omega\text{-m}$

$G^w$  is an adimensional coefficient, 0.1356.

$\langle J_s \rangle$  is the average magnetic polarization,  $\langle J_s \rangle = 0.85 \cdot 2.15$

$H_{\text{hist}}$  is the coercive field,  $H_{\text{hist}} = P_{\text{hist}} \cdot d / 4 \cdot B_{\text{max}} \cdot f$

$d$  is density,  $7850 \text{ kg/m}^3$

From that we got an anomalous loss of 13 W/kg, which is a significant part of the total loss, but cannot explain all parasitic losses. So, we must assume that there is a significant fraction of classic parasitic loss, but we cannot calculate it precisely because we do not have a good estimate of the “effective particle size”. It should be possible, in the future, to establish a relation between sample resistivity and the “effective particle size”.

### Conclusions

- It was not possible to achieve the density values mentioned in the literature. Density increases with compaction pressure even in the range 700-900 MPa. The maximum value was around  $7.2 \text{ g/cm}^3$ .
- Increasing compaction pressure up to 600 MPa decreased resistivity, due to increased particle connectivity. It did not change from 600 to 800 MPa.
- Resistivity decreased as heat treatment temperature increased, but peak values were obtained around  $230^\circ\text{C}$ .
- The positive effect of density increase on permeability is stronger than the expected from an increase in saturation magnetization, and is probably related to the demagnetizing fields associated with pores.
- Compaction pressures from 700 to 900 MPa did not alter significantly the DC hysteresis loop area or the 400 Hz total loss values. The DC hysteresis energy dissipation is ten times higher than the typical values for electrical steel sheets.
- Hysteresis loss component accounts for 70% of total losses at 400Hz. Classic parasitic losses and anomalous losses calculated by the conventional equations cannot account for the 35 W/kg of parasitic losses.
- Classic parasitic losses should not be estimated by using either the composite electrical resistivity or the particle size, because it renders unreasonable low values of parasitic losses. An “effective interconnected particle size” should be taken into account.

### Acknowledgments

The authors would like to thank FAPESP (97/04877-0) and FAPERGS for the financial support of this work. We also would like to thank Mr. Francis Hanejko from Hoeganaes Corporation for providing technical data and samples of powder.

### References

- [1] F. G. Hanejko, H. G. Phan, H. G. Rutz, T. L. Stuart Powder Metallurgy Materials for AC Magnetic Applications. Hoeganaes Technical Data. Presented at PM<sup>2</sup>TEC'96 World Congress, June, Washington D.C., 1996.
- [2] B. Kordecki, B. Weglinski, J. Kaczmar Properties and Applications of Soft Magnetic Composites. *Powder Metallurgy*, v.25, no.4, 1982, p.-201-208.
- [3] C. Gélinas, J. Battison, J. M. Iron-Resin Composite Materials for AC Magnetic Applications. 1998 PM World Congress.
- [4] P. Janson Soft Magnetic Composites – from DC to MHz with Iron Powder. 1998 PM World Congress.
- [5] M. Hiroyki, H. Yagushi, Y. Seki Magnetic Properties of Dust Cores Made from Iron Powder with Insulating Inorganic Compound Coating. PM 1998 World Congress.
- [6] G. Ban, G. Bertotti Dependence on Peak Induction and Grain Size of Power Losses in Nonoriented SiFe Steels. *J. Appl. Phys.*, v. 64, 1988, p. 5361-5363.

## **Advanced Powder Technology II**

10.4028/www.scientific.net/KEM.189-191

## **Properties of Iron Powder for AC Magnetic Application**

10.4028/www.scientific.net/KEM.189-191.649